Nitroxyl (HNO) Reacts with Molecular Oxygen and Forms Peroxynitrite at Physiological pH

BIOLOGICAL IMPLICATIONS*[S]

Renata Smulik[‡], **Dawid Dębski**[‡], **Jacek Zielonka**[§], **Bartosz Michałowski**[‡], **Jan Adamus**[‡], **Andrzej Marcinek**[‡], **Balaraman Kalyanaraman**[§1], and **Adam Sikora**[‡2]

From the [‡]Institute of Applied Radiation Chemistry, Lodz University of Technology, 90-924 Lodz, Poland and the [§]Department of Biophysics and Free Radical Research Center, Medical College of Wisconsin, Milwaukee, Wisconsin 53226

Background: Nitroxyl (HNO) is a reactive nitrogen species implicated in cardioprotection.
Results: Nitroxyl reacts with oxygen to form an oxidizing and nitrating species, peroxynitrite.
Conclusion: In the presence of oxygen, HNO donors may be a source of peroxynitrite.
Significance: Peroxynitrite formation should be taken into account in the extracellular milieu when exposing cells to HNO donor under aerobic conditions.

Nitroxyl (HNO), the protonated one-electron reduction product of NO, remains an enigmatic reactive nitrogen species. Its chemical reactivity and biological activity are still not completely understood. HNO donors show biological effects different from NO donors. Although HNO reactivity with molecular oxygen is described in the literature, the product of this reaction has not yet been unambiguously identified. Here we report that the decomposition of HNO donors under aerobic conditions in aqueous solutions at physiological pH leads to the formation of peroxynitrite (ONOO$^-$) as a major intermediate. We have specifically detected and quantified ONOO$^-$ with the aid of boronate probes, e.g. coumarin-7-boronic acid or 4-boronobenzyl derivative of fluorescein methyl ester. In addition to the major phenolic products, peroxynitrite-specific minor products of oxidation of boronate probes were detected under these conditions. Using the competition kinetics method and a set of HNO scavengers, the value of the second order rate constant of the HNO reaction with oxygen ($k = 1.8 \times 10^4$ M^{-1} s^{-1}) was determined. The rate constant ($k = 2 \times 10^4$ M^{-1} s^{-1}) was also determined using kinetic simulations. The kinetic parameters of the reactions of HNO with selected thiols, including cysteine, dithiothreitol, N-acetylcysteine, captopril, bovine and human serum albumins, and hydrogen sulfide, are reported. Biological and cardiovascular implications of nitroxyl reactions are discussed.

Nitroxyl (HNO), the protonated one-electron reduction product of NO, remains an enigmatic reactive nitrogen species. Its chemical reactivity and biological activity are still not completely understood. HNO donors show biological effects different from NO donors.

Nitroxyl (1, 2) (HNO; nitrosyl hydride in the IUPAC nomenclature),[3] the protonated form of one-electron reduction product of nitric oxide (•NO), still remains a mysterious reactive nitrogen species. In the past, its chemistry received much less attention than the chemistry of other reactive nitrogen species (e.g. •NO, nitrogen dioxide radical (•NO$_2$), and peroxynitrite (ONOO$^-$)).

Significant and important pharmacological effects associated with the use of nitroxyl donors have been reported. It has been shown that HNO generated from Angeli's salt acts as a vasorelaxant (3–8). We reported that inclusion of Angeli's salt in cardioplegic solution improved myocardial functional recovery during ischemia and reperfusion in isolated rat hearts (9, 10). We attributed cardioprotection to either nitric oxide (•NO) or nitrous oxide (N$_2$O) generated from nitroxyl anion (NO$^-$). Because nitronyl nitroxides (also PTIO) reversed this cardioprotective effect, we proposed that •NO generated directly or indirectly from Angeli's salt was responsible for vasorelaxation and cardioprotection. Additional research is needed to increase our understanding of the chemical biology and reactivity of HNO (11, 12). Several studies examining HNO *in vitro* demonstrated that Angeli's salt (HNO donor) exerts marked cytotoxicity that is oxygen-dependent (13–16).

The endogenous production of HNO in mammalian systems has not been unambiguously shown to occur; however, there is considerable *in vitro* evidence for the intermediacy of this species from HNO donors. It has been suggested that HNO can be formed from •NO synthases via the oxidation of N$^\omega$-hydroxy-L-

[3] The abbreviations used are: HNO, nitroxyl; CBA, coumarin-7-boronic acid; COH, 7-hydroxycoumarin; CPTIO, 2-(4-carboxyphenyl)-4,4,5,5-tetramethylimidazoline-1-oxyl-3-oxide; DPTA-NONOate, ((Z)-1-[N-(3-aminopropyl)-N-(3-ammoniopropyl)-amino]diazen-1-ium-1,2-diolate); dtpa, diethylenetriaminepentaacetic acid; FBBE, 7-benzylboronic derivative of fluorescein methyl ester; FME, fluorescein methyl ester; iPrOH, isopropanol; MitoPh, benzyltriphenylphosphonium cation; ONOO$^-$, peroxynitrite, p-MitoPhB(OH)$_2$, (4-boronobenzyl)-triphenylphosphonium cation; p-MitoPhOH, (4-hydroxybenzyl)-triphenylphosphonium cation; p-MitoPhNO$_2$, (4-nitrobenzyl)-triphenylphosphonium cation; PMT, photomultiplier; PTIO, 2-phenyl-4,4,5,5-tetramethylimidazoline-1-oxyl-3-oxide; TEMPOL, 4-hydroxy-2,2,6,6-tetramethylpiperidine-1-oxyl; UPLC, ultra performance liquid chromatography.
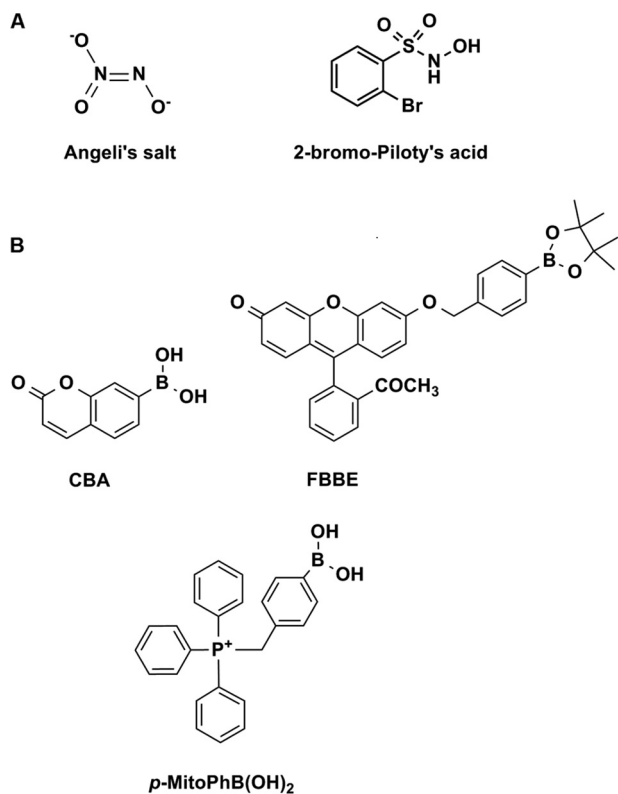
FIGURE 1. **Chemical structures of HNO donors (*A*) and the boronate probes (*B*) used in this study.**

arginine (17–19). Moreover, it has been shown *in vitro* that HNO can be formed via the reduction of $^{\bullet}$NO by mitochondrial cytochrome *c*, xanthine oxidase, or ubiquinol (2, 20–22). Reports indicate that HNO is also presumably formed from nitrosothiol reaction with other thiols or ascorbate (23, 24). Although based on kinetic considerations, their biological relevance remains doubtful (23, 24).

More recently, new fluorescent probes for quantitative detection of HNO in aqueous solution were reported (25, 26). The ground state of HNO is a singlet, but NO^- anion, which is formed upon HNO deprotonation, similarly to the isoelectronic O_2 molecule, has the triplet ground state. HNO is a weak acid ($pK_a = 11.4$) (27), and its deprotonation is a spin-forbidden reaction and an exceptionally slow process. It has been reported that nitroxyl anion (NO^-) reacts very quickly with molecular oxygen forming peroxynitrite.

$$NO^- + O_2 \rightarrow ONOO^-$$
<div align="center">REACTION 1</div>
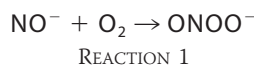
In the absence of scavengers, HNO spontaneously dimerizes in aqueous solutions with the second order rate constant of $k = 8 \times 10^6 \ M^{-1} \ s^{-1}$ to yield hyponitrous acid, which upon water elimination yields N_2O (28).

$$2HNO \rightarrow [HONNOH] \rightarrow N_2O + H_2O$$
<div align="center">REACTION 2</div>

The most frequently used HNO donors are Angeli's salt and Piloty's acid or its derivatives (29) (Fig. 1*A*). HNO is highly reactive toward thiols, which are considered major targets of this molecule in biological systems (30–32). Moreover, HNO is capable of reacting with metals and metalloproteins (*e.g.* superoxide dismutase, HRP, catalase, and cytochrome *c*) (33–39). Although the high reactivity of HNO toward cellular thiols and metal centers could classify this species as a potential signaling molecule (32), the lack of information concerning its endogenous biosynthetic pathways questions its biological relevance. Nitroxides and nitronyl nitroxides are also commonly used HNO scavengers (36, 40, 41).

One of the most intriguing aspects of nitroxyl (HNO/NO^-) chemistry is its reaction with molecular oxygen (42–46). It is commonly accepted that the reaction between nitroxyl anion (NO^-) and molecular oxygen leads to the formation of $ONOO^-$ (45, 46). Despite numerous studies on the reactivity of HNO with molecular oxygen, the product of this reaction has not been unequivocally identified (42, 44). The possibility of peroxynitrite formation from the reaction between HNO and O_2 remained skeptical and understudied (42, 44). This is, in part, due to the lack of availability of specific probes that directly react with $ONOO^-$ to form specific diagnostic products. Here, we present unambiguous evidence for $ONOO^-$ formation during the reaction between HNO and molecular oxygen using the recently developed assays for specific detection and quantification of peroxynitrite (47, 48).

We have reported previously that boronic acids and their esters react directly and rapidly with $ONOO^-$ ($k = 10^6 \ M^{-1}$ s^{-1}), with the formation of corresponding phenols as major products (85–90%) (49). Although boronates also react with H_2O_2, the rate of reaction is rather sluggish ($k = \sim 1 \ M^{-1} \ s^{-1}$). An array of pro-fluorescent boronate-based probes has been reported, providing now the opportunity for noninvasive, real time monitoring and imaging of $ONOO^-$ in cell-free and cellular systems (50–54). In this study two profluorescent probes (CBA and FBBE) and a nonfluorescent probe, phenylboronic acid with a bulky triphenylphosphonium group (*p*-MitoPhB $(OH)_2$) (47) were used (Fig. 1*B*). The reaction between $ONOO^-$ and boronate leads to the formation of $ONOO^-$ adduct, followed by the cleavage of the O-O bond, which may proceed via a nonradical, major pathway (heterolytic cleavage of O-O bond) or radical-mediated, minor pathway (homolytic cleavage of the O-O bond). The minor pathway yields unique nitrated products that are highly specific for $ONOO^-$ reaction with boronate. The detailed mechanism of the reaction of boronates with $ONOO^-$ has been recently reported (47, 48). We demonstrated that the formation of the products of both major and minor pathways in a specific ratio can be used as a "peroxynitrite fingerprint" and applied this strategy to unambiguously determine the identity of the product of the reaction of HNO with molecular oxygen.

EXPERIMENTAL PROCEDURES

Chemicals—Boronate probes CBA and *p*-MitoPhB$(OH)_2$ were synthesized according to the published procedure (50, 55). FBBE was synthesized by benzylation of fluorescein methyl ester (FME) with the use of 4-(iodomethyl)phenylboronic acid pinacol ester.[4] In all experiments Angeli's salt was used as a

---

[4] K. Dębowska, D. Dębski, B. Michałowski, J. Adamus, and A. Sikora, manuscript in preparation.

HNO donor, synthesized according to the published procedure (29). The concentration of Angeli's salt stock solutions was determined by measuring the absorbance at 248 nm ($\epsilon = 8.3 \times 10^3$ M^{-1} s^{-1}) (29) in 1 mM aqueous NaOH solutions. Another HNO donor, 2-bromo-N-hydroxybenzenesulfonamide, was synthesized according to the published procedure (56). Peroxynitrite was prepared according to the published procedure (57), by reacting nitrite with H_2O_2. The concentration of $ONOO^-$ was determined by measuring the absorbance at 302 nm ($\epsilon = 1.7 \times 10^3$ M^{-1} s^{-1}) (57) in 1 mM aqueous NaOH solutions. Stock solution of hydrogen sulfide was prepared by dissolving sodium sulfide in water. HNO scavengers, and all other reagents (of the highest purity available) were obtained from Sigma-Aldrich, whereas DPTA-NONOate was purchased from Cayman Chemicals, and catalase was from Boehringer. Each solution was prepared using deionized water (Millipore Milli-Q system).

UV-visible Absorption Measurements—The UV-visible absorption spectra were collected with Agilent 8453 spectrophotometer equipped with photodiode array detector and thermostated (25 °C) cell holder.

Stopped Flow Measurements—Stopped flow kinetics experiments were performed using Applied Photophysics SX 20 stopped flow spectrophotometer equipped with a fluorescence detector. Angeli's salt (3 μM in 1 mM NaOH) was rapidly mixed with the solution containing CBA (25 μM), phosphate buffer (25 mM, pH 7.4), dtpa (50 μM), 5% CH_3CN, and HNO scavenger (at an appropriate concentration). The reaction mixtures were excited at 332 nm, and the emitted light intensity was measured at 470 nm (PMT voltage = 850 V, emission/excitation slit = 2.5 nm). The thermostated cell (25 °C) with a 10-mm optical pathway was used for kinetic measurements.

Fluorescence Measurements—Fluorescence measurements were performed using Varian Cary Eclipse spectrofluorometer equipped with a plate reader accessory. The solutions containing FBBE were excited at 494 nm, and the emitted light intensity was measured at 518 nm (PMT voltage = 580 V, emission slit = 2.5 nm, excitation slit = 5 nm). Reactions were performed at room temperature. Typically, the boronate probe (25 μM) was incubated in phosphate buffer (50 mM, pH 7.4), dtpa (100 μM), 5% CH_3CN, and HNO donor and scavenger (at the appropriate concentration), and the extent of FBBE oxidation to FME was monitored over time.

UPLC/MS Analyses—Boronate probes and products of their oxidative conversion were analyzed using Acquity UPLC (Waters) system coupled online with LCT Premier XE (Waters) mass spectrometer with a time-of-flight mass detector. One microliter of sample was injected into the UPLC system equipped with the C_{18} column (Waters Aquity BEH C18, 100 × 2.1 mm, 1.7 μm) maintained at 40 °C and equilibrated with 30% CH_3CN (containing 0.1% (v/v) TFA) in 0.1% TFA solution. The compounds were separated by a linear increase of CH_3CN concentration in mobile phase from 30 to 60% using a flow rate of 0.35 ml/min. Under these conditions, the following retention times were observed: CBA, 2.79 min; COH, 3.04 min; coumarin (CH), 3.66 min; 7-nitrocoumarin (CNO_2), 3.86 min; p-MitoPhB $(OH)_2$, 2.75 min; p-MitoPhOH, 3.10 min; p-MitoPhNO$_2$, 3.71 min; MitoPh, 3.91 min. The compounds were detected and

quantified by monitoring the absorption at 300 ± 5 nm for CBA solutions and 268 ± 5 nm for p-MitoPhB$(OH)_2$ solutions, respectively. The mass spectrometer was operated in W mode with a lock mass correction. Lock mass solution (leucine-enkephalin, reference mass: $[M + H]^+_{C12}$ 556.2771; $[M + H]^+_{C13}$ 557.2801) was prepared at a concentration of 0.5 ng/μl in 50:50 (v/v), water/acetonitrile solution and stored in 4 °C until further use. Data acquisition was performed using a MassLynx 4.1 data software (Waters).

Deoxygenation and Oxygenation of CBA and Angeli's Salt Solution—Samples consisting of 250 μM CBA and 200 μM Angeli's salt were incubated in phosphate buffer (50 mM, pH 7.4) containing dtpa (100 μM) for 90 min at 25 °C under vacuum or purged with O_2 to obtain anaerobic and O_2-saturated solutions, respectively.

Determination of $O_2^{\bar{}}$ and $^{\bullet}NO$ Fluxes—$^{\bullet}NO$ fluxes were determined from the measured rate of the decomposition of DPTA-NONOate by following the decrease in its characteristic absorbance at 250 nm ($\epsilon = 8 \times 10^3$ M^{-1} s^{-1}) (58, 59). This rate was multiplied by a factor of 2 to obtain the rate of $^{\bullet}NO$ release (assuming that two molecules of $^{\bullet}NO$ are released from one molecule of DPTA-NONOate). The flux of $O_2^{\bar{}}$ was determined by monitoring of cytochrome reduction following the increase in absorbance at 550 nm (using molar absorption coefficient of 2.1×10^4 M^{-1} s^{-1}) (60).

Kinetic Simulations—The kinetic simulation was carried out using a freely available software, Kintecus 4.55 (61). The kinetic model used in this study is a modification of the published model (62). The list of the chemical reactions, rate constants, and major modifications used in the simulation is shown in supplemental Table S1.

RESULTS

The Oxidation of CBA Probe in O_2-saturated Angeli's Salt Solutions—Angeli's salt slowly decomposed at pH 7.4, releasing HNO. As shown in Fig. 2*A*, its decay resulted in the disappearance of the absorption band maximum at 235 nm. In the presence of CBA the decomposition of Angeli's salt was accompanied by 7-hydroxycoumarin (COH) formation as reflected by the disappearance of the absorption band of boronate probe at 287 nm and the build-up of absorption of COH at 370 nm (Fig. 2*B*). The kinetics of CBA decay and COH appearance mirror the dynamics of Angeli's salt decomposition observed in the absence of CBA (Fig. 2*C*). These data indicate that decomposition of Angeli's salt resulted in the formation of an oxidant capable of rapid conversion of CBA probe into COH. The other HNO donor, 2-bromo-N-hydroxybenzenesulfonamide, also oxidized CBA in the same manner as Angeli's salt (data not shown).

To test the possibility of the formation of $ONOO^-$ via the reaction of HNO with O_2, it was essential to confirm that Angeli's salt itself does not trigger the oxidation of CBA. As expected, neither COH formation was observed in the absence of Angeli's salt (Fig. 3, *line d*) nor in the absence of oxygen (Fig. 3, *line c*). Similar yields of COH were observed when CBA was incubated with Angeli's salt in aerated (*line b*) or oxygenated (*line a*) conditions. These data indicate that both HNO and molecular oxygen are essential for oxidative conversion of boronate probe. Only a minimal increase was observed after the
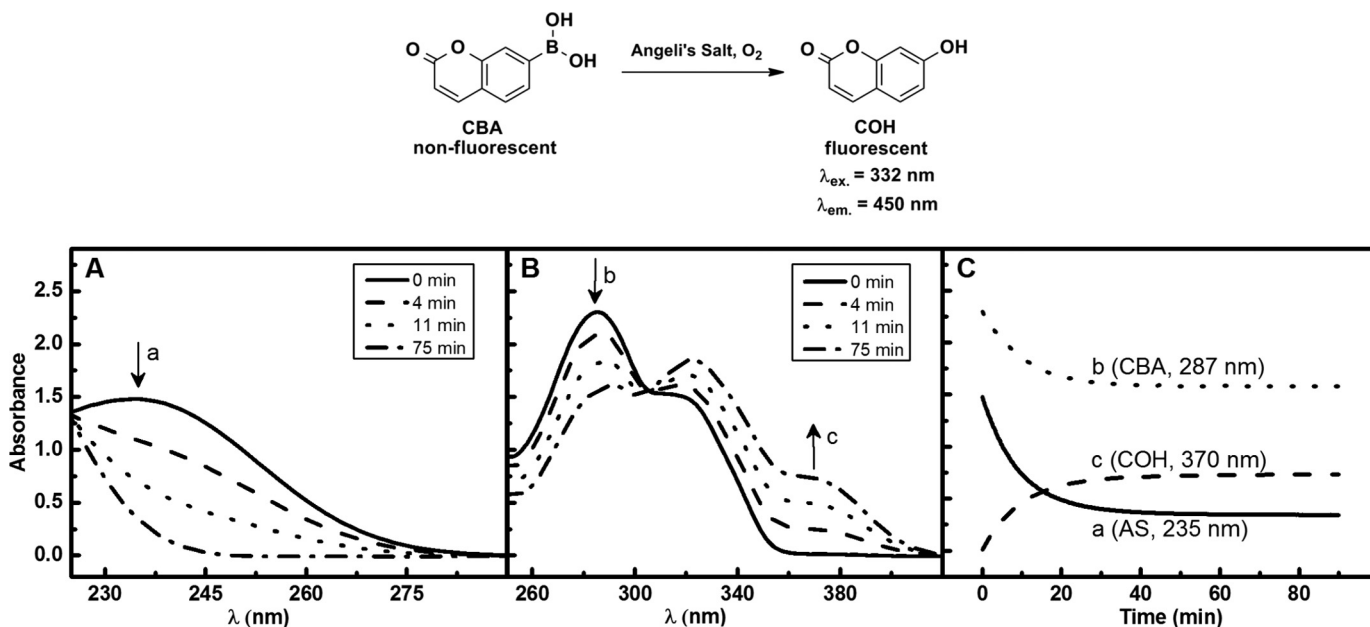
FIGURE 2. *A* and *B*, spectral changes observed during decomposition of Angeli's salt alone (*A*) and Angeli's salt-induced oxidation of CBA to COH (*B*). *C*, comparison of the kinetics of decomposition of Angeli's salt alone and of Angeli's salt-induced conversion of CBA to COH. Incubation mixture consisted of 150 μM Angeli's salt in phosphate buffer (pH 7.4, 50 mM) containing dtpa (100 μM) and 5% CH$_3$CN (without CBA, *A*; or with CBA 100 μM, *B*). The decay kinetics of Angeli's salt and CBA were monitored spectroscopically at 235 and 287 nm, respectively. The COH formation kinetic trace was recorded at 370 nm.
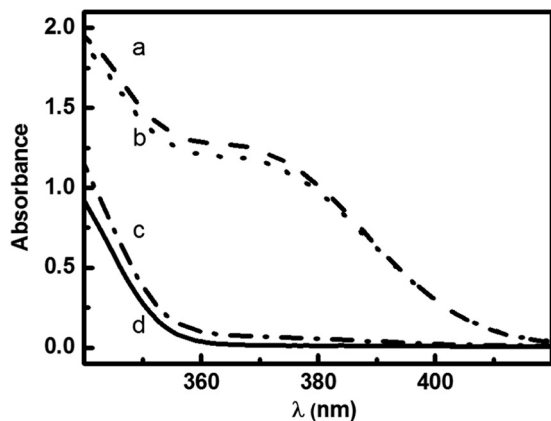

FIGURE 3. **The effect of oxygen on COH formation from Angeli's salt-induced oxidation of CBA.** Incubation mixtures consisted of 250 μM CBA and 200 μM Angeli's salt (*lines a–c*) in phosphate buffer (pH 7.4, 50 mM) containing dtpa (100 μM), 5% CH$_3$CN, and the spectra were recorded after 1.5 h of incubation at 25 °C. *Line a*, O$_2$-saturated solution; *line b*, solution in equilibrium with the air; *line c*, solution deaerated using vacuum; *line d*, solution without Angeli's salt addition.

~5-fold increase in O$_2$ concentration (from 20% O$_2$ in air to 100% O$_2$).

Profiling of CBA Products Formed in Aqueous Solutions of Angeli's Salt: UPLC Study—For detailed characterization of oxidant formed in the reaction between HNO and molecular oxygen, the profiles of major and minor oxidation products of CBA were examined. For qualitative and quantitative determination of these products, we used the UPLC analysis. As shown in Fig. 4, in the presence of authentic ONOO$^-$, CBA was converted to COH as the major product, and coumarin and 7-nitrocoumarin (CNO$_2$) as minor products formed in the radical pathway. This result is consistent with previous reports for simple arylboronates (49) and mitochondria-targeted boronate probes (47). Replacement of the boronate moiety in boronic

compounds by the nitro group strongly supports an intermediary role of peroxynitrite (47, 48). Mechanism of the reaction of CBA with ONOO$^-$ is shown in Fig. 5. The profile of products formed during Angeli's salt-induced oxidation closely resembles the profile observed for ONOO$^-$-induced oxidation of CBA (Fig. 4). The addition of glutathione, a known scavenger of HNO, almost completely inhibited oxidation of boronate probe in the solutions containing Angeli's salt, but not when a bolus ONOO$^-$ was used. Although glutathione is known to react with peroxynitrite ($k = 1.36 \times 10^3$ M^{-1} s^{-1}) (63), 100 μM GSH cannot compete with 100 μM CBA probe for ONOO$^-$ (the rate constant of the CBA reaction with peroxynitrite is equal to $k = 1.1 \times 10^6$ M^{-1} s^{-1}) (50).

The quantitative analysis of substrate depletion and product formation during the incubation of CBA probe in aerated Angeli's salt solution and in the reaction between CBA and authentic ONOO$^-$, added as bolus or generated from superoxide and nitric oxide fluxes, is shown in Fig. 6.

Previous studies indicated that neither O$_2^{\bar{\cdot}}$ produced by xanthine/xanthine oxidase, nor ·NO (DPTA-NONOate), caused the oxidation of boronate. Only ONOO$^-$ generated *in situ* from these systems was able to cause an oxidative conversion of the probe (47, 49, 50, 52).

The titration profiles are very similar for ONOO$^-$ and for Angeli's salt, indicating that the reaction between HNO and molecular oxygen results in the formation of ONOO$^-$, which reacts rapidly with CBA ($k = 1.1 \times 10^6$ M^{-1} s^{-1}) yielding COH as a major product (50) and the minor products formed via the radical pathway (Fig. 5).

As shown previously (47), the ratios of rate constants for the radical (k_r) and nonradical (k_{nr}) pathways can be determined from the plot of the sum of the concentrations of minor products *versus* the concentration of the major, phenolic product. Fig. 6 shows the k_r/k_{nr} ratio determined for CBA oxidation.

Clearly, the oxidation of CBA probe in the aerated solution of Angeli's salt and in xanthine/xanthine oxidase/DPTA NONO-ate system results in the same product formation profiles and

FIGURE 4. **The chromatograms recorded during UPLC analyses of products formed during oxidation of CBA by peroxynitrite and Angeli's salt.** Incubation mixtures consisted of 100 μM CBA in phosphate buffer (pH 7.4, 50 mM) containing dtpa (100 μM), catalase (100 units/ml), 10% iPrOH, and peroxynitrite or Angeli's salt and glutathione at the indicated concentrations. CBA and its corresponding oxidation products were detected using UV absorption detection at 300 $\pm$ 5 nm.

equal k_r/k_{nr} ratio. The yields of both major (COH) and minor (coumarin and CNO_2) products were the same (within the experimental error) for Angeli's salt- and $O_2^-/\cdot NO$-induced oxidation of CBA (Table 1). The oxidative transformation of CBA by peroxynitrite added as bolus leads to the higher yield of COH and, as a consequence, a lower k_r/k_{nr} ratio. A possible explanation of that phenomenon is the formation of peroxynitrate (O_2NOO^-) in the reaction between $ONOO^-$ and its protonated form (ONOOH) at the high local concentration of $ONOO^-$, when added by bolus addition (64). Peroxynitrate anion is also able to oxidize CBA to COH (data not shown), but not through the radical pathway.

As discussed previously, the profile of the products formed from the reaction between peroxynitrite and boronate probes is highly specific for this oxidant, providing a "peroxynitrite fingerprint." Therefore, the similar profiles of the products formed during the peroxynitrite (both bolus and generated *in situ* from co-generated O_2^- and $\cdot NO$ fluxes) and Angeli's salt-dependent oxidation of CBA, both qualitatively and quantitatively (Table 1) provide strong evidence that the oxidant formed during the reaction between HNO and molecular oxygen is $ONOO^-$.

Because the minor products of CBA oxidation by $ONOO^-$ have not been previously identified, we used another boronate probe, *p*-MitoPhB(OH)$_2$ (47), from which the minor products of reaction with $ONOO^-$ have been well characterized (47). The detailed mechanism of the reaction of this probe with $ONOO^-$ is similar to the previously mentioned CBA oxidation mechanism (Fig. 5) (49). The major pathway leads to the formation of corresponding phenol (*p*-MitoPhOH), whereas under the conditions used the minor pathway yields two products: MitoPh (dominant) and *p*-MitoPhNO$_2$. Titration of *p*-MitoPhB(OH)$_2$ probe with Angeli's salt results in the product profiles shown in Fig. 7, indicating the formation of both phenolic (major) and radical-mediated products (minor). The profiles of the product formation resemble the profiles described previously for authentic peroxynitrite (47). Detection of $ONOO^-$-specific products using two different boronate probes in aerobic reaction mixtures of Angeli's salt undoubtedly shows that the reaction of HNO with O_2 leads to formation of peroxynitrite.
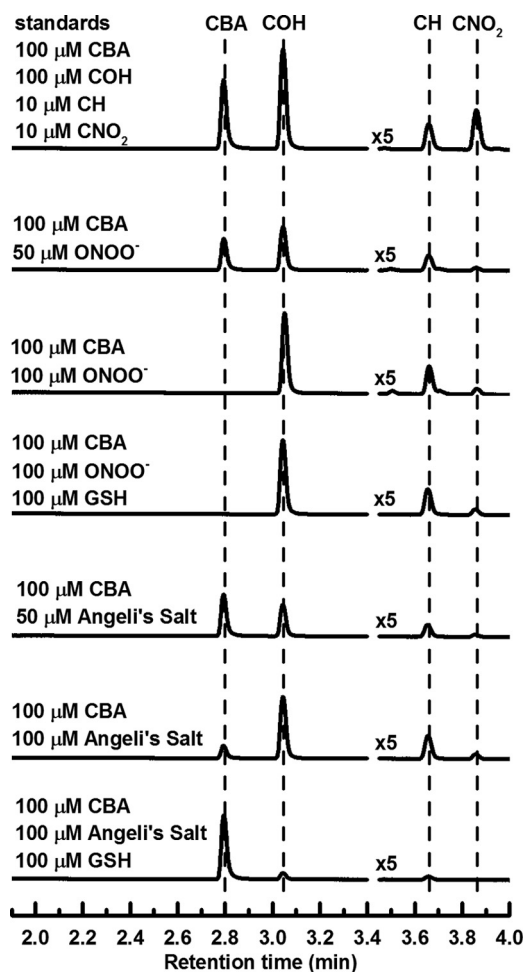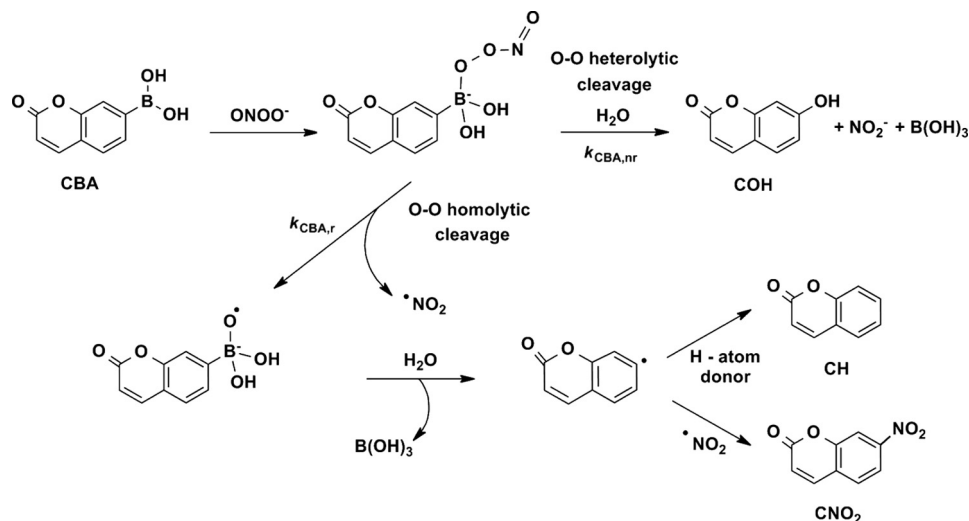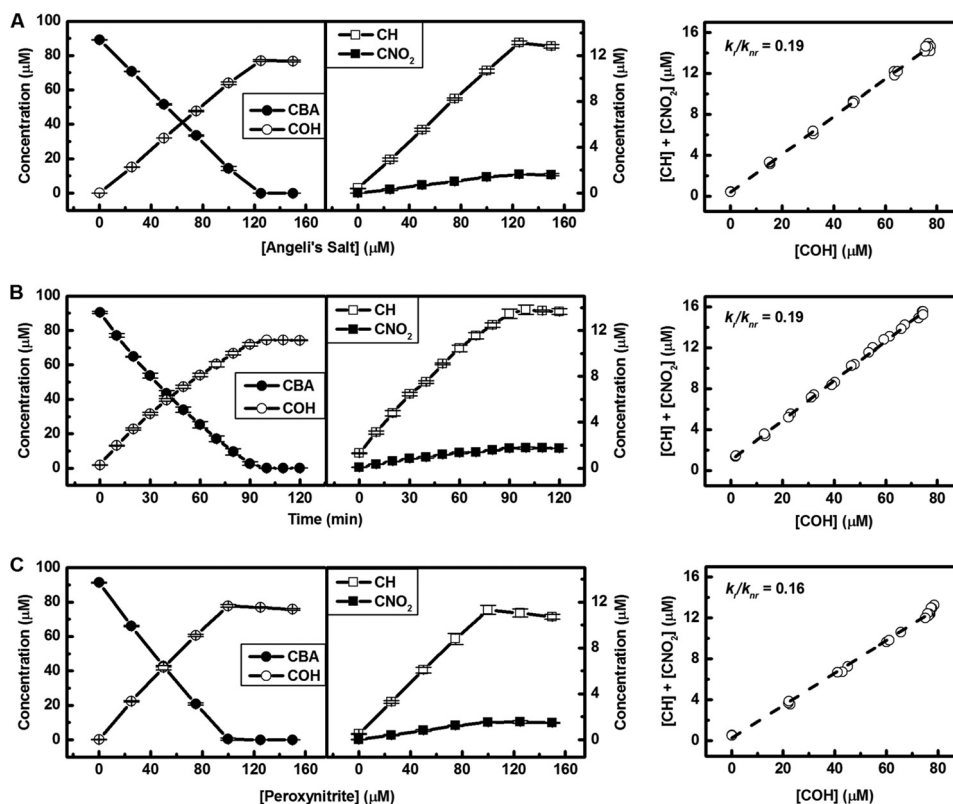

FIGURE 5. **The mechanism of the reaction between ONOO$^-$ and CBA.**

FIGURE 6. **Relationship between substrate depletion and major/minor product formation during Angeli's salt (*A*) or peroxynitrite titration of CBA solutions (*C*) and xanthine/xanthine oxidase/DPTA NONOate-induced oxidation of CBA (*B*) over the time.** Incubation mixtures consisted of 90 μM CBA in phosphate buffer (pH 7.4, 50 mM) containing dtpa (100 μM), catalase (100 units/ml), 10% iPrOH, and Angeli's salt/peroxynitrite at the indicated concentration. After 1.5 of incubation at 25 °C of Angeli's salt or bolus addition of peroxynitrite, the reaction mixtures were analyzed using the UPLC/UV method. CBA and its corresponding oxidation products were detected using UV absorption detection at 300 ± 5 nm. Each point represents the average value of three samples. The ratio of the rate constants of homolytic (*radical, k_r*) and heterolytic (*nonradical, k_{nr}*) cleavage pathways was estimated. Xanthine (1 mM) and xanthine oxidase (2.25 milliunits/ml) were mixed and added to 600 μM DPTA-NONOate in phosphate buffer (pH 7.4, 50 mM) containing CBA (90 μM), dtpa (100 μM), catalase (100 units/ml), and 10% iPrOH, resulting in 1.55 ± 0.05 μM/min superoxide and >1.6 μM/min nitric oxide flux at 25 °C. CBA and its corresponding oxidation products were detected and analyzed as previously.

TABLE 1

Yields of products formed upon oxidation of CBA in different systems yielding peroxynitrite

Angeli's salt (0–160 μM) was incubated for 1.5 h at 25 °C in the solution of 90 μM of CBA in phosphate buffer (pH 7.4, 50 mM) containing dtpa (100 μM), catalase (100 units/ml), and 10% iPrOH. Xanthine (1 mM) and xanthine oxidase (2.25 milliunits/ml) were mixed and added to 600 μM DPTA-NONOate in phosphate buffer (pH 7.4, 50 mM) containing CBA (90 μM), dtpa (100 μM), catalase (100 units/ml), and 10% iPrOH, resulting in 1.55 ± 0.05 μM/min superoxide and >1.6 μM/min nitric oxide flux at 25 °C. ONOO$^-$ (0–160 μM) added by bolus addition to phosphate buffer (pH 7.4, 50 mM) containing 90 μM of CBA dtpa (100 μM), catalase (100 units/ml), and 10% iPrOH. The presented yields represent the average values of three independent experiments. The Student's t test was used to determine the statistical significance of differences for presented values of products yields.

	COH	Coumarin	CNO$_2$
	%	*%*	*%*
Angeli's salt	83.8 ± 0.2	14.4 ± 0.2	1.8 ± 0.2
X/XO/DPTA NONOate	82.7 ± 0.3	15.3 ± 0.2	2.0 ± 0.1
ONOO− bolus addition	85.8 ± 0.3[a]	12.5 ± 0.3[a]	1.7 ± 0.1

[a] p values of < 0.005 were considered as significant.

Determination of the Rate Constant of the Reaction of HNO with Oxygen—To determine the second order rate constant of the reaction between HNO and molecular oxygen, the competition kinetics approach was used. In this study, the HNO dimerization was not taken under consideration as in the aerated aqueous solutions, and at low Angeli's salt concentration (0–10 μM) this process is negligible. In fact, a 5-fold increase in oxygen concentration did not enhance the extent of CBA oxidation to COH (Fig. 3), indicating that reaction with oxygen outcompetes the self-decomposition of nitroxyl. HNO released from Angeli's salt reacts with molecular oxygen and HNO scavengers, when they are present (Fig. 8). Reaction of HNO with molecular oxygen leads to the formation of peroxynitrite, and there are two pathways of peroxynitrite-derived CBA oxidation (Fig. 5). The nonradical (*nr*) pathway of that reaction leads to the formation of COH, and the rate of COH accumulation over time is expressed by Equation 1,

$$v = \frac{d[\text{COH}]}{dt} = k_{\text{CBA,nr}}[\text{CBA}][\text{ONOO}^-] \qquad \text{(Eq. 1)}$$

where $k_{\text{CBA,nr}}$ is the rate constant for the nonradical pathway of CBA oxidation. Changes in the concentrations of HNO and ONOO$^-$ over time are expressed by Equations 2 and 3,

$$\frac{d[\text{HNO}]}{dt} = k_{\text{AS}}[\text{AS}] - k_{\text{S}}[\text{S}][\text{HNO}] - k_{\text{O}_2}[\text{O}_2][\text{HNO}]$$

$$\text{(Eq. 2)}$$

$$\frac{d[\text{ONOO}^-]}{dt} = k_{\text{O}_2}[\text{O}_2][\text{HNO}]$$

$$- k_{\text{CBA,nr}}[\text{CBA}][\text{ONOO}^-] - k_{\text{CBA,r}}[\text{CBA}][\text{ONOO}^-] \quad \text{(Eq. 3)}$$
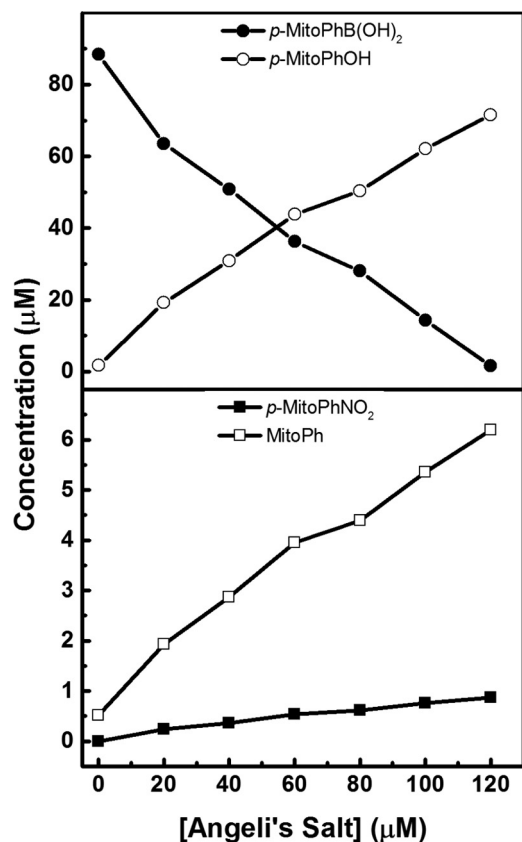
FIGURE 7. **Relationship between substrate depletion and major/minor product formation during the Angeli's salt-induced oxidation of *p*-MitoPhB(OH)₂.** Incubation mixtures consisted of 90 μM *p*-MitoPhB(OH)₂ in phosphate buffer (pH 7.4, 50 mM) containing dtpa (100 μM), catalase (100 units/ml), 10% iPrOH, and Angeli's salt at the indicated concentrations. After 15 min of incubation at 40 °C with Angeli's salt, the reaction mixtures were analyzed using the UPLC/UV method. *p*-MitoPhB(OH)₂ and its corresponding oxidation products were detected using UV absorption detection at 268 ± 5 nm. Each point represents the aver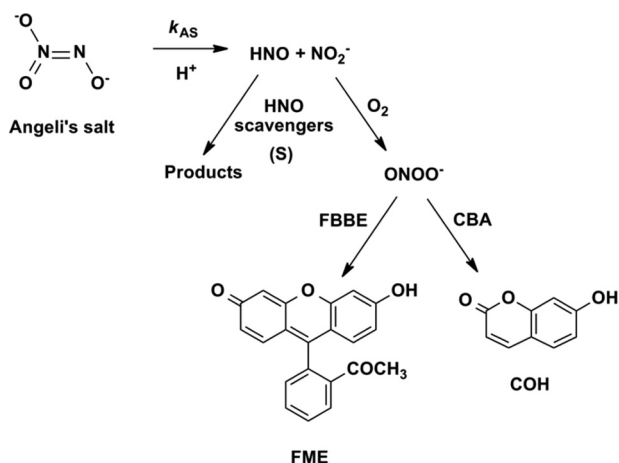age value of three samples. The concentrations were determined based on the calibration curves obtained for the authentic standards.

FIGURE 8. **Reaction model used for the determination of the rate constant of the reaction between HNO and oxygen using competition kinetics approach.** *S*, scavenger.

where k_{AS} is the rate constant of Angeli's salt decomposition, and k_S and k_{O2} are the constants of HNO reactions with scavenger and molecular oxygen, respectively. The rate constant $k_{CBA,r}$ is the constant for the radical (r) pathway of CBA reac-

tion with peroxynitrite. To solve the equations steady state approximation was made (Equation 1.4).

$$\frac{d[\text{ONOO}^-]}{dt} = \frac{d[\text{HNO}]}{dt} = 0 \qquad \text{(Eq. 4)}$$

Finally, the solution of aforementioned equations leads to Equations 5 and 6.

$$[\text{HNO}] = \frac{k_{AS}[\text{AS}]}{k_S[\text{S}] + k_{O_2}[O_2]} \qquad \text{(Eq. 5)}$$

$$[\text{ONOO}^-] = \frac{k_{O_2}[O_2]}{(k_{CBA,nr} + k_{CBA,r})[\text{CBA}]}[\text{HNO}] \qquad \text{(Eq. 6)}$$

The initial rate of the COH formation is expressed by Equation 7, whereas in the absence of HNO scavenger it is expressed by relationship Equation 8.

$$v_i = \frac{k_{CBA,nr}}{k_{CBA,nr} + k_{CBA,r}} k_{AS}[\text{AS}] \frac{k_{O_2}[O_2]}{k_S[\text{S}]_1 + k_{O_2}[O_2]} \qquad \text{(Eq. 7)}$$

$$v_0 = \frac{k_{CBA,nr}}{k_{CBA,nr} + k_{CBA,r}} k_{AS}[\text{AS}] \qquad \text{(Eq. 8)}$$

Comparison of the equations expressing initial rates results in Equation 9.

$$\frac{v_0}{v_i} = 1 + \frac{k_S [\text{S}]_i}{K_{O_2}[O_2]} \qquad \text{(Eq. 9)}$$

The ratios of the rate constants of the second order reaction of HNO with its scavenger (k_S) and molecular oxygen (k_{O2}) were estimated using Equation 9. Two fluorogenic probes, CBA and FBBE, were used, which upon oxidation yield blue fluorescent (COH) and green fluorescent (FME) products, respectively (Fig. 8). In this survey, an excess of boronate probe (25 μM CBA or FBBE) was used over Angeli's salt (3 or 10 μM) and HNO scavenger (0–10 μM). The oxidation products of those two probes are fluorescent; therefore, changes in the initial rate of the formation of the corresponding phenols were monitored with the use of spectrofluorometer or the stopped flow spectrophotometer. As shown in Fig. 9 (*A* and *B*), the addition of glutathione, an efficient HNO scavenger, inhibits the initial rates of oxidation of both probes. The kinetic traces were obtained from at least two independent measurements. A linear function was fitted to data obtained within first 3 min of steady state measurements (Fig. 9, *B* and *E*). In the stopped flow experiments, the initial period of the reaction was reduced to 60 s. The results were plotted *versus* the ratio of the HNO scavenger to oxygen concentration (225 μM) and fitted linearly. The slope of the *dashed lines* in Fig. 9 (*C* and *F*) is equal to the value of the ratio of rate constants of the reactions of HNO with glutathione and with molecular oxygen.

The values of the second order rate constant published in the literature for the reaction of HNO with molecular oxygen vary. Liochev and Fridovich (31) estimated that this rate constant equaled $\approx 1 \times 10^4$ M^{-1} s^{-1}, whereas others reported the rate constant to be $\sim 3 \times 10^3$ M^{-1} s^{-1} (36). We calculated the values of the k_{O2} from the k_S/k_{O2} ratios obtained experimen-
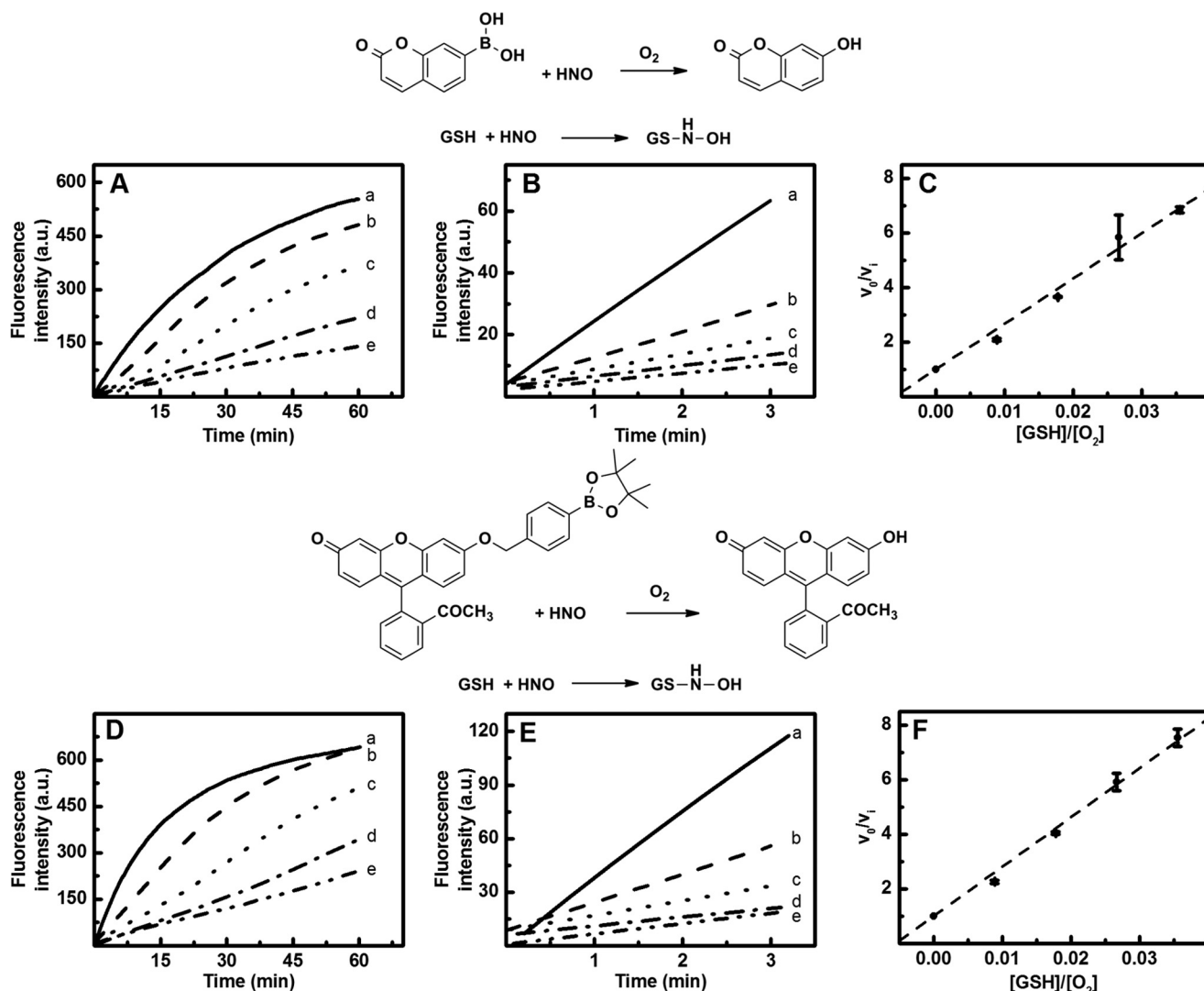
FIGURE 9. **The effect of glutathione on the initial rate of corresponding phenol formation from the boronate probes.** *A*, incubation mixture consisted of CBA (25 μM), Angeli's salt (10 μM), and GSH (*line a*, 0 μM; *line b*, 2 μM; *line c*, 4 μM; *line d*, 6 μM; *line e*, 10 μM) in phosphate buffer (pH 7.4, 25 mM) containing dtpa (50 μM). *D*, incubation mixture consisted of FBBE (25 μM), Angeli's salt (10 μM), and GSH (*line a*, 0 μM; *line b*, 2 μM; *line c*, 4 μM; *line d*, 6 μM; *line e*, 10 μM) in phosphate buffer (pH 7.4, 25 mM) containing dtpa (50 μM). *B* and *E*, initial period of the reaction presented in *A* or *D*, respectively. *C* and *F*, the effect of glutathione on the initial rate of COH or fluorescein methyl ester formation, respectively. The solutions containing CBA were excited at 332 nm, and the emitted light intensity was measured at 470 nm (PMT voltage = 585 V, emission/excitation slit = 5 nm), whereas the solutions containing FBBE were excited at 494 nm, and the emitted light intensity was measured at 518 nm (PMT voltage = 580 V, emission slit = 2.5 nm, excitation slit = 5 nm). Each point represents the average value of two samples. The *error bars* represent standard deviations.

tally using the published rate constants for selected scavengers of HNO (CPTIO, PTIO, TEMPOL, superoxide dismutase, and HRP) (36, 40, 41). From obtaining the mean of values (Table 2), we determined this rate constant to be $\sim(1.8 \pm 0.3) \times 10^4$ M^{-1} s^{-1}.

Reactivity of HNO toward Thiols—Next, we determined the rate constants for the reactions between HNO and selected thiols. The calculated values of the rate constant of selected thiols are shown in Table 3. With small molecular weight thiols (except H$_2$S), there is a correlation between the rate constants and pK_a values of SH groups. The higher the value of pK_a, the lower the reaction rate constant of HNO with thiol. The rate constants for the reactions of HNO with glutathione and with *N*-acetylcysteine have been previously reported (2×10^6 and 5×10^5 M^{-1} s^{-1}, respectively) (36). Our analysis leads to similar but slightly higher values of the rate constants of HNO scavenging, namely $3.1 \pm 0.6 \times 10^6$ M^{-1} s^{-1} for glutathione and $1.4 \pm 0.3 \times 10^6$ M^{-1} s^{-1} for *N*-acetylcysteine (Table 3).

Kinetic Simulations—The value of the rate constant of HNO reaction with O$_2$ was also determined by kinetic simulations, which mirrored the kinetic experiments. In computational calculations, we were changing the value of k_{O_2} to find the best fit of the computed values of k_S/k_{O_2} ratios to the experimental values. The resulting values of second order rate constant for the reaction of HNO with molecular oxygen are presented in the Table 2, and the averaged value is equal to 2×10^4 M^{-1} s^{-1}. In the reaction with HNO all selected scavengers: CPTIO, PTIO, TEMPOL, superoxide dismutase, and HRP yield nitric oxide, which subsequently reacts with nitroxyl (Reaction 3, $k = (5.8 \pm 0.4) \times 10^6$ M^{-1} s^{-1}) (27).

TABLE 2

The determined values of the k_S/k_{O_2} ratio (average value of three independent experiments; pH 7.4, 25 °C) for selected HNO scavengers and the calculated values of k_{O_2}

Compound	k_S/k_{O_2}	k_S	$k_{O_2}{}^a \times 10^{-4}$	$k_{O_2}{}^b \times 10^{-4}$
		$M^{-1}\,s^{-1}$	$M^{-1}\,s^{-1}$	$M^{-1}\,s^{-1}$
CPTIO	6.9 ± 0.1^c	$(1.4 \pm 0.2) \times 10^5$ (40)	(2.0 ± 0.3)	2.2
	6.8 ± 0.1^d		(2.1 ± 0.3)	2.1
PTIO	8.3 ± 0.2^c	$(1.4 \pm 0.2) \times 10^5$ (40)	(1.7 ± 0.3)	1.8
	10.5 ± 0.5^d		(1.3 ± 0.3)	1.4
TEMPOL	8.1 ± 0.2^c	$(1.4 \pm 0.2) \times 10^5$ (41)	(1.7 ± 0.3)	2.0
	9 ± 1^d		(1.6 ± 0.4)	1.6
SOD	28 ± 1^c	7×10^5 (36)	2.5	2.8
	36 ± 2^d		1.9	2.0
HRP	125 ± 1^d	2×10^6 (36)	1.6	1.8
Mean values		$k_{O_2}{}^a = (1.8 \pm 0.3) \times 10^4\,M^{-1}\,s^{-1}$		
		$k_{O_2}{}^b = (2.0 \pm 0.4) \times 10^4\,M^{-1}\,s^{-1}$		

[a] Value of k_{O_2} obtained by dividing k_S from the literature by the determined k_S/k_{O_2} ratio.
[b] Value of k_{O_2} obtained from kinetic simulations.
[c] Steady state measurements.
[d] Stopped flow measurements.

TABLE 3

The determined values of the k_S/k_{O_2} ratio (average value of three independent experiments; pH 7.4, 25 °C) for selected HNO scavengers and the calculated values of k_S

Compound	k_S/k_{O_2}	$k_S \times 10^{-6a}$	$k_S \times 10^{-6b}$	pK_a (reference)
		$M^{-1}\,s^{-1}$	$M^{-1}\,s^{-1}$	
Thiols				
Cysteine	244 ± 7^c	4.5 ± 0.9	5.0	8.3 (67)
Glutathione	171 ± 1^c	3.1 ± 0.6	3.5	8.8 (67)
Dithiothreitol	155 ± 9^c	2.8 ± 0.7	3.2	9.1 (67)
N-Acetylcysteine	75 ± 1^c	1.4 ± 0.3	1.5	9.5 (67)
Captopril	33 ± 1^c	0.6 ± 0.1	0.7	9.8 (67)
H_2S	63 ± 3^c	1.2 ± 0.3	1.3	7.05 (68)
Proteins				
BSA	75 ± 2^c	1.4 ± 0.3	1.5	7.86–8.00 (69)
HSA	79 ± 8^c	1.4 ± 0.4	1.6	8.6 (70)

[a] Value of k_S obtained by multiplying determined k_S/k_{O_2} ratio by $k_{O_2}{}^a$ in Table 2 = $(1.8 \pm 0.3) \times 10^4\,M^{-1}\,s^{-1}$.
[b] Value of k_S obtained by multiplying determined k_S/k_{O_2} ratio by $k_{O_2}{}^b$ in Table 2 = $(2.0 \pm 0.4) \times 10^4\,M^{-1}\,s^{-1}$ obtained from kinetic simulations.
[c] Stopped flow measurements.

$$HNO + {}^\bullet NO \rightarrow HN_2O_2^-$$

REACTION 3

Because this reaction cannot be separated from experimentally observed effect of HNO scavengers, the obtained k_{O_2} rate constant differs from the value obtained via classical kinetic analysis. Similar simulations were performed to determine the rate constants of HNO reaction with thiols (cysteine, glutathione, dithiothreitol, *N*-acetylcysteine, and captopril), bovine and human serum albumin, and HS⁻. In these simulations, the rate constant for the reaction of HNO with O_2 was set to be equal to $2 \times 10^4\,M^{-1}\,s^{-1}$. During kinetic simulation, we were changing the value of k_S to get the best agreement with experimentally determined k_S/k_{O_2} ratios. The calculated rate constants are presented in Table 3. Fig. 10 (*A* and *B*) shows the comparison of the experimentally recorded increase of fluorescence corresponding to CBA oxidation to COH and the simulated kinetic traces of COH build-up for two HNO scavengers: TEMPOL and glutathione.

DISCUSSION

Chemical Considerations—Here we have shown that ONOO⁻ is the major product of the reaction between HNO and molecular oxygen. Previously Miranda (42) has shown that Angeli's salt, like ONOO⁻, is able to oxidize dihydrorhodamine in the presence of oxygen. However, the structure of the reactive oxidant

formed from the reaction between HNO and molecular oxygen was not characterized. It was also shown that Angeli's salt, unlike ONOO⁻, is unable to oxidize phenols to their dimeric and fluorescent products. This led to the conclusion that ONOO⁻ is not formed in the reaction of HNO with molecular oxygen, and different products of the reaction of HNO with O_2 were proposed (42). However, the dimeric phenols are formed via recombination of phenoxyl radicals. Because phenoxyl radicals are moderate one-electron oxidants, they can be readily reduced by HNO formed in this system. Contrary to Miranda (42), Kirsch and de Groot (43) have shown that ONOO⁻ and oxidant formed in aerated solutions of Angeli's salt exhibit a similar pattern of the reactivity, suggesting formation of peroxynitrite in the reaction of HNO with O_2. Several studies examining HNO *in vitro* demonstrated that Angeli's salt (HNO donor) exerted marked and oxygen-dependent cytotoxicity (13–16). The present results show that ONOO⁻ is formed as a major product from HNO reaction with O_2, and thus, the cytotoxicity of HNO donors can be at least partially explained through formation of peroxynitrite.

The rate constant for the reaction of HNO with molecular oxygen was determined to be ~$(1.8 \pm 0.3) \times 10^4\,M^{-1}\,s^{-1}$ at pH 7.4, and this value is two times higher than the reported value by Liochev and Fridovich *et al.* (31) ($8 \times 10^3\,M^{-1}\,s^{-1}$) and approximately five times higher than the value proposed by other authors (36) ($3 \times 10^3\,M^{-1}\,s^{-1}$). Based on the rate constant
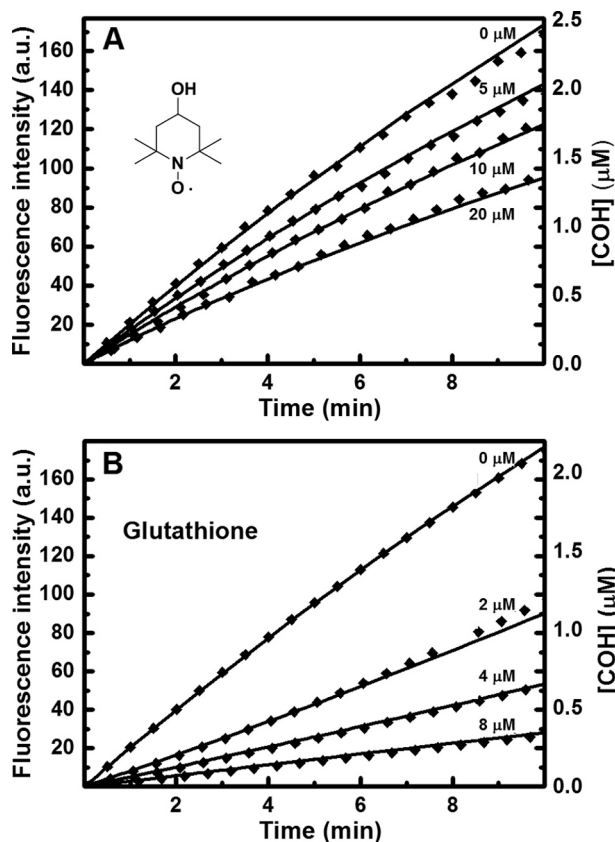
FIGURE 10. **The effect of HNO scavengers on the oxidative conversion of CBA into COH by ONOO⁻ formed in the reaction of HNO with molecular oxygen: the comparison of experimental data with the kinetic simulation.** The experimental conditions were as follows: *A*, CBA (25 μM), Angeli's salt (10 μM), TEMPOL (0 μM, 5 μM, 10 μM, 20 μM), phosphate buffer (pH 7.4, 50 mM), dtpa (100 μM), and O_2 (225 μM). *B*, CBA (25 μM), Angeli's salt (10 μM), GSH (0 μM, 2 μM, 4 μM, 8 μM), phosphate buffer (pH 7.4, 50 mM), and dtpa (100 μM), O_2 (225 μM). The *points* represent the measured fluorescence intensity, and *solid lines* represent the calculated COH concentrations.

determined for the reaction of HNO with O_2 and the kinetic model used, we evaluated the rate constants of the reactions of HNO with selected thiols of possible biological and/or pharmacological relevance. The proposed methodology is easy to conduct and could be used for further HNO reactivity assessment. As previously shown for glutathione, we observed that other thiols also react with HNO significantly faster than does molecular oxygen, with the rate constants 2 orders of magnitude higher. These results indicate that it is very unlikely that HNO would react with O_2 in the intracellular milieu, because of the high content of reduced thiols (both low molecular and proteins) and relatively low concentration of oxygen in most tissues. However, the reaction of HNO with O_2 may be important in well oxygenated biological systems under decreased content of reduced thiols (for example under oxidative stress conditions). In addition, this reaction should be taken into account during *in vitro* studies, when exposing cells to HNO donor under aerobic conditions.

Biological Considerations—Recently, the potential beneficial actions of Angeli's salt in failing rat hearts were attributed to concomitant vasodilation and inotropic mechanism via soluble guanylyl cyclase-dependent and -independent mechanisms (65). The cardioprotective effect (*e.g.* enhanced contractile

function) of HNO donor (CXL-1020) in patients with heart failure was recently demonstrated (66). CXL-1020 is synthesized from Piloty's acid and decomposes to HNO more slowly than Angeli's salt (66). Published results show that CXL-1020 decomposes to form N_2O through a mechanism similar to that of Angeli's salt (66). Although CXL-1020 was shown to be safe and well tolerated in patients with heart failure (66), prolonged administration of this drug at slightly higher doses caused inflammatory reactions in dogs (66). The authors indicated that this toxic side effect could derail its use as a human therapeutic (66). Based on the present results, it is abundantly clear that in the presence of oxygen, HNO donors will form ONOO⁻ as a major intermediate in the extracellular milieu. This finding may be relevant in explaining their toxic side effects.

REFERENCES

1. Fukuto, J. M., Bartberger, M. D., Dutton, A. S., Paolocci, N., Wink, D. A., and Houk, K. N. (2005) The physiological chemistry and biological activity of nitroxyl (HNO): The neglected, misunderstood, and enigmatic nitrogen oxide. *Chem. Res. Toxicol.* **18,** 790–801
2. Miranda, K. M. (2005) The chemistry of nitroxyl (HNO) and implications in biology. *Coord. Chem. Rev.* **249,** 433–455
3. Fukuto, J. M., Chiang, K., Hszieh, R., Wong, P., and Chaudhuri, G. (1992) The pharmacological activity of nitroxyl: a potent vasodilator with activity similar to nitric oxide and/or endothelium-derived relaxing factor. *J. Pharmacol. Exp. Ther.* **263,** 546–551
4. Ellis, A., Li, C. G., and Rand, M. J. (2000) Differential actions of L-cysteine on responses to nitric oxide, nitroxyl anions and EDRF in the rat aorta. *Br. J. Pharmacol.* **129,** 315–322
5. Wanstall, J. C., Jeffery, T. K., Gambino, A., Lovren, F., and Triggle, C. R. (2001) Vascular smooth muscle relaxation mediated by nitric oxide donors: a comparison with acetylcholine, nitric oxide and nitroxyl ion. *Br. J. Pharmacol.* **134,** 463–472
6. Irvine, J. C., Favaloro, J. L., Widdop, R. E., and Kemp-Harper, B. K. (2007) Nitroxyl anion (HNO) donor, Angeli's salt, does not develop tolerance *in vivo*. *Hypertension* **49,** 885–892
7. Irvine, J. C., Favaloro, J. L., and Kemp-Harper, B. K. (2003) NO⁻ activates soluble guanylate cyclase and K-v channels to vasodilate resistance arteries. *Hypertension* **41,** 1301–1307
8. Favaloro, J. L., and Kemp-Harper, B. K. (2007) The nitroxyl anion (HNO) is a potent dilator of rat coronary vasculature. *Cardiovasc. Res.* **73,** 587–596
9. Joseph, J., Konorev, E., Baker, J., and Kalyanaraman, B. (1994) Nitronyl nitroxides inhibit the vasorelaxation induced by Angeli salt (sodium trioxodinitrate) in myocardium. *FASEB J.* **8,** A313
10. Joseph, J., Konorev, E. A., Singh, R. J., Hogg, N., and Kalyanaraman, B. (1996) Myocardial protection with nitroxyl (NO⁻) and nitric oxide (NO) donors. *Biochemistry* **35,** 9287–9308
11. Irvine, J. C., Ritchie, R. H., Favaloro, J. L., Andrews, K. L., Widdop, R. E., and Kemp-Harper, B. K. (2008) Nitroxyl (HNO): the Cinderella of the nitric oxide story. *Trends Pharmacol. Sci.* **29,** 601–608
12. Switzer, C. H., Flores-Santana, W., Mancardi, D., Donzelli, S., Basudhar, D., Ridnour, L. A., Miranda, K. M., Fukuto, J. M., Paolocci, N., and Wink, D. A. (2009) The emergence of nitroxyl (HNO) as a pharmacological agent. *Biochim. Biophys. Acta* **1787,** 835–840
13. Augustyniak, A., Skolimowski, J., and Blaszczyk, A. (2013) Cytotoxicity of nitroxyl (HNO/NO⁻) against normal and cancer human cells. *Chem. Biol. Interact.* **206,** 262–271
14. Hewett, S. J., Espey, M. G., Uliasz, T. F., and Wink, D. A. (2005) Neurotoxicity of nitroxyl: Insights into HNO and NO biochemical imbalance. *Free Radic. Biol. Med.* **39,** 1478–1488
15. Stoyanovsky, D. A., Schor, N. F., Nylander, K. D., and Salama, G. (2004) Effects of pH on the cytotoxicity of sodium trioxodinitrate (Angeli's salt). *J. Med. Chem.* **47,** 210–217
16. Chazotte-Aubert, L., Oikawa, S., Gilibert, I., Bianchini, F., Kawanishi, S.,

and Ohshima, H. (1999) Cytotoxicity and site-specific DNA damage induced by nitroxyl anion (NO⁻) in the presence of hydrogen peroxide: Implications for various pathophysiological conditions. *J. Biol. Chem.* **274,** 20909 –20915

17. Pagliaro, P. (2003) Differential biological effects of products of nitric oxide (NO) synthase: it is not enough to say NO. *Life Sci.* **73,** 2137–2149

18. Pufahl, R. A., Wishnok, J. S., and Marletta, M. A. (1995) Hydrogen peroxide-supported oxidation of *N*ω-hydroxy-L-arginine by nitric oxide synthase. *Biochemistry* **34,** 1930 –1941

19. Hobbs, A. J., Fukuto, J. M., and Ignarro, L. J. (1994) Formation of free nitric oxide from l-arginine by nitric oxide synthase: direct enhancement of generation by superoxide dismutase. *Proc. Natl. Acad. Sci. U.S.A.* **91,** 10992–10996

20. Sharpe, M. A., and Cooper, C. E. (1998) Reactions of nitric oxide with mitochondrial cytochrome c: a novel mechanism for the formation of nitroxyl anion and peroxynitrite. *Biochem. J.* **332,** 9–19

21. Saleem, M., and Ohshima, H. (2004) Xanthine oxidase converts nitric oxide to nitroxyl that inactivates the enzyme. *Biochem. Biophys. Res. Commun.* **315,** 455– 462

22. Poderoso, J. J., Carreras, M. C., Schöpfer, F., Lisdero, C. L., Riobó, N. A., Giulivi, C., Boveris, A. D., Boveris, A., and Cadenas, E. (1999) The reaction of nitric oxide with ubiquinol: kinetic properties and biological significance. *Free Radic. Biol. Med.* **26,** 925–935

23. Kirsch, M., Büscher, A. M., Aker, S., Schulz, R., and de Groot, H. (2009) New insights into the *S*-nitrosothiol-ascorbate reaction: the formation of nitroxyl. *Org. Biomol. Chem.* **7,** 1954 –1962

24. Wong, P. S., Hyun, J., Fukuto, J. M., Shirota, F. N., DeMaster, E. G., Shoeman, D. W., and Nagasawa, H. T. (1998) Reaction between *S*-nitrosothiols and thiols: generation of nitroxyl (HNO) and subsequent chemistry. *Biochemistry* **37,** 5362–5371

25. Mao, G. J., Zhang, X. B., Shi, X. L., Liu, H. W., Wu, Y. X., Zhou, L. Y., Tan, W. H., and Yu, R. Q. (2014) A highly sensitive and reductant-resistant fluorescent probe for nitroxyl in aqueous solution and serum. *Chem. Commun. (Camb.).* **50,** 5790 –5792

26. Wrobel, A. T., Johnstone, T. C., DelizLiang, A., Lippard, S. J., and Rivera-Fuentes, P. (2014) A fast and selective near-infrared fluorescent se-nsor for multicolor imaging of biological nitroxyl (HNO). *J. Am. Chem. Soc.* **136,** 4697– 4705

27. Shafirovich, V., and Lymar, S. V. (2002) Nitroxyl and its anion in aqueous solutions: Spin states, protic equilibria, and reactivities toward oxygen and nitric oxide. *Proc. Natl. Acad. Sci. U.S.A.* **99,** 7340 –7345

28. Shafirovich, V., and Lymar, S. V. (2003) Spin-forbidden deprotonation of aqueous nitroxyl (HNO). *J. Am. Chem Soc.* **125,** 6547– 6552

29. Hughes, M. N., and Cammack, R. (1999) Synthesis, chemistry, and applications of nitroxyl ion releasers sodium trioxodinitrate or Angeli's salt and Piloty's acid. *Methods Enzymol.* **301,** 279 –287

30. Fukuto, J. M., Bianco, C. L., and Chavez, T. A. (2009) Nitroxyl (HNO) signaling. *Free Radic. Biol. Med.* **47,** 1318 –1324

31. Liochev, S. I., and Fridovich, I. (2003) The mode of decomposition of Angeli's salt (Na₂N₂O₃) and the effects thereon of oxygen, nitrite, superoxide dismutase, and glutathione. *Free Radic. Biol. Med.* **34,** 1399 –1404

32. Fukuto, J. M., Cisneros, C. J., and Kinkade, R. L. (2013) A comparison of the chemistry associated with the biological signaling and actions of nitroxyl (HNO) and nitric oxide (NO). *J. Inorg. Biochem.* **118,** 201–208

33. Murphy, M. E., and Sies, H. (1991) Reversible conversion of itroxyl anion to nitric-oxide by superoxide-dismutase. *Proc. Natl. Acad. Sci. U.S.A.* **88,** 10860 –10864

34. Liochev, S. I., and Fridovich, I. (2001) Copper, zinc superoxide dismutase as a univalent NO⁻ oxidoreductase and as a dichlorofluorescin peroxidase. *J. Biol. Chem.* **276,** 35253–35257

35. Liochev, S. I., and Fridovich, I. (2002) Nitroxyl (NO⁻): a substrate for superoxide dismutase. *Arch. Biochem. Biophys.* **402,** 166 –171

36. Miranda, K. M., Paolocci, N., Katori, T., Thomas, D. D., Ford, E., Bartberger, M. D., Espey, M. G., Kass, D. A., Feelisch, M., Fukuto, J. M., and Wink, D. A. (2003) A biochemical rationale for the discrete behavior of nitroxyl and nitric oxide in the cardiovascular system. *Proc. Natl. Acad. Sci. U.S.A.* **100,** 9196 –9201

37. Bazylinski, D. A., and Hollocher, T. C. (1985) Metmyoglobin and methe-

moglobin as efficient traps for nitrosyl hydride (nitroxyl) in neutral aqueous-solution. *J. Am. Chem. Soc.* **107,** 7982–7986

38. Doyle, M. P., Mahapatro, S. N., Broene, R. D., and Guy, J. K. (1988) Oxidation and reduction of hemoproteins by trioxodinitrate (II): the role of nitrosyl hydride and nitrite. *J. Am. Chem. Soc.* **110,** 593–599

39. Suarez, S. A., Marti, M. A., De Biase, P. M., Estrin, D. A., Bari, S. E., and Doctorovich, F. (2007) HNO trapping and assisted decomposition of nitroxyl donors by ferric hemes. *Polyhedron* **26,** 4673– 4679

40. Samuni, U., Samuni, Y., and Goldstein, S. (2010) On the distinction between nitroxyl and nitric oxide using nitronyl nitroxides. *J. Am. Chem. Soc.* **132,** 8428 – 8432

41. Samuni, Y., Samuni, U., and Goldstein, S. (2013) The use of cyclic nitroxide radicals as HNO scavengers. *J. Inorg. Biochem.* **118,** 155–161

42. Miranda, K. M., Espey, M. G., Yamada, K., Krishna, M., Ludwick, N., Kim, S., Jourd'heuil, D., Grisham, M. B., Feelisch, M., Fukuto, J. M., and Wink, D. A. (2001) Unique oxidative mechanisms for the reactive nitrogen oxide species, nitroxyl anion. *J. Biol. Chem.* **276,** 1720 –1727

43. Kirsch, M., and de Groot, H. (2002) Formation of peroxynitrite from reaction of nitroxyl anion with molecular oxygen. *J. Biol. Chem.* **277,** 13379 –13388

44. Miranda, K. M., Yamada, K., Espey, M. G., Thomas, D. D., DeGraff, W., Mitchell, J. B., Krishna, M. C., Colton, C. A., and Wink, D. A. (2002) Further evidence for distinct reactive intermediates from nitroxyl and peroxynitrite: effects of buffer composition on the chemistry of Angeli's salt and synthetic peroxynitrite. *Arch. Biochem. Biophys.* **401,** 134 –144

45. Donald, C. E., Hughes, M. N., Thompson, J. M., and Bonner, F. T. (1986) Photolysis of the N=N bond in trioxodinitrate: reaction between triplet NO⁻ and O₂ to form peroxonitrite. *Inorg. Chem.* **25,** 2676 –2677

46. Samuni, A., and Goldstein, S. (2011) One-electron oxidation of acetohydroxamic acid: the intermediacy of nitroxyl and peroxynitrite. *J. Phys. Chem. A* **115,** 3022–3028

47. Sikora, A., Zielonka, J., Adamus, J., Debski, D., Dybala-Defratyka, A., Michalowski, B., Joseph, J., Hartley, R. C., Murphy, M. P., and Kalyanaraman, B. (2013) Reaction between peroxynitrite and triphenylphosphonium-substituted arylboronic acid isomers: identification of diagnostic marker products and biological implications. *Chem. Res. Toxicol.* **26,** 856– 867

48. Sikora, A., Zielonka, J., Lopez, M., Dybala-Defratyka, A., Joseph, J., Marcinek, A., and Kalyanaraman, B. (2011) Reaction between peroxynitrite and boronates: EPR spin-trapping, HPLC Analyses, and quantum mechanical study of the free radical pathway. *Chem. Res. Toxicol.* **24,** 687– 697

49. Sikora, A., Zielonka, J., Lopez, M., Joseph, J., and Kalyanaraman, B. (2009) Direct oxidation of boronates by peroxynitrite: mechanism and implications in fluorescence imaging of peroxynitrite. *Free Radic. Biol. Med.* **47,** 1401–1407

50. Zielonka, J., Sikora, A., Joseph, J., and Kalyanaraman, B. (2010) Peroxynitrite is the major species formed from different flux ratios of co-generated nitric oxide and superoxide: direct reaction with boronate-based fluorescent probe. *J. Biol. Chem.* **285,** 14210 –14216

51. Zielonka, J., Sikora, A., Hardy, M., Joseph, J., Dranka, B. P., and Kalyanaraman, B. (2012) Boronate probes as diagnostic tools for real time monitoring of peroxynitrite and hydroperoxides. *Chem. Res. Toxicol.* **25,** 1793–1799

52. Zielonka, J., Zielonka, M., Sikora, A., Adamus, J., Joseph, J., Hardy, M., Ouari, O., Dranka, B. P., and Kalyanaraman, B. (2012) Global profiling of reactive oxygen and nitrogen species in biological systems: high-throughput real-time analyses. *J. Biol. Chem.* **287,** 2984 –2995

53. Sieracki, N. A., Gantner, B. N., Mao, M., Horner, J. H., Ye, R. D., Malik, A. B., Newcomb, M. E., and Bonini, M. G. (2013) Bioluminescent detection of peroxynitrite with a boronic acid-caged luciferin. *Free Radic. Biol. Med.* **61,** 40 –50

54. Lippert, A. R., Van de Bittner, G. C., and Chang, C. J. (2011) Boronate oxidation as a bioorthogonal reaction approach for studying the chemistry of hydrogen peroxide in living systems. *Acc. Chem. Res.* **44,** 793– 804

55. Morrison, D. E., Issa, F., Bhadbhade, M., Groebler, L., Witting, P. K., Kassiou, M., Rutledge, P. J., and Rendina, L. M. (2010) Boronated phosphonium salts containing arylboronic acid, closo-carborane, or nido-carborane: synthesis, X-ray diffraction, in vitro cytotoxicity, and cellular uptake.

J. Biol. Inorg. Chem. **15,** 1305–1318

56. Cline, M. R., Tu, C., Silverman, D. N., and Toscano, J. P. (2011) Detection of nitroxyl (HNO) by membrane inlet mass spectrometry. *Free Radic. Biol. Med.* **50,** 1274–1279

57. Bohle, D. S., Glassbrenner, P. A., and Hansert, B. (1996) Synthesis of pure tetramethylammonium peroxynitrite. *Methods Enzymol.* **269,** 302–311

58. Goss, S. P., Hogg, N., and Kalyanaraman, B. (1997) The effect of nitric oxide release rates on the oxidation of human low density lipoprotein. *J. Biol. Chem.* **272,** 21647–21653

59. Hrabie, J. A., Klose, J. R., Wink, D. A., and Keefer, L. K. (1993) New nitric oxide-releasing zwitterions derived from polyamines. *J. Org. Chem.* **58,** 1472–1476

60. Massey, V. (1959) The microestimation of succinate and the extinction coefficient of cytochrome-c. *Biochim. Biophys. Acta* **34,** 255–256

61. Ianni, J. C. (2003) A comparison of the Bader-Deuflhard and the Cash-Karp Runge-Kutta integrators for the GRI-MECH 3.0 model based on the chemical kinetics code kintecus. In *Computational Fluid and Solid Mechanics*, pp. 1368–1372, Elsevier Science Ltd., Oxford, UK

62. Kirsch, M., Korth, H. G., Wensing, A., Sustmann, R., and de Groot, H. (2003) Product formation and kinetic simulations in the pH range 1–14 account for a free-radical mechanism of peroxynitrite decomposition. *Arch. Biochem. Biophys.* **418,** 133–150

63. Alvarez, B., and Radi, R. (2003) Peroxynitrite reactivity with amino acids and proteins. *Amino Acids* **25,** 295–311

64. Gupta, D., Harish, B., Kissner, R., and Koppenol, W. H. (2009) Peroxynitrate is formed rapidly during decomposition of peroxynitrite at neutral pH. *Dalton Trans.* **29,** 5730–5736

65. Chin, K. Y., Qin, C., Cao, N., Kemp-Harper, B. K., Woodman, O. L., and Ritchie, R. H. (2014) The concomitant coronary vasodilator and positive inotropic actions of the nitroxyl donor Angeli's salt in the intact rat heart: contribution of soluble guanylyl cyclase-dependent and -independent mechanisms. *Br. J. Pharmacol.* **171,** 1722–1734

66. Sabbah, H. N., Tocchetti, C. G., Wang, M., Daya, S., Gupta, R. C., Tunin, R. S., Mazhari, R., Takimoto, E., Paolocci, N., Cowart, D., Colucci, W. S., and Kass, D. A. (2013) Nitroxyl (HNO): a novel approach for the acute treatment of heart failure. *Circ. Heart Fail.* **6,** 1250–1258

67. Winterbourn, C. C., and Metodiewa, D. (1999) Reactivity of biologically important thiol compounds with superoxide and hydrogen peroxide. *Free Radic. Biol. Med.* **27,** 322–328

68. Ellis, A. J., and Milestone, N. B. (1967) Ionization constants of hydrogen sulphide from 20 to 90 degrees C. *Geochim. Cosmochim. Acta* **31,** 615–620

69. Radi, R., Beckman, J. S., Bush, K. M., and Freeman, B. A. (1991) Peroxynitrite oxidation of sulfhydryls: the cytotoxic potential of superoxide and nitric-oxide. *J. Biol. Chem.* **266,** 4244–4250

70. Radi, R., Alvarez, B., Ferrer-Sueta, G., and Freeman, B. A. (1999) Kinetics of peroxynitrite reaction with amino acids and human serum albumin. *J. Biol. Chem.* **274,** 842–848